OPEN ACCESS

University of BRISTOL

Peer reviewed version

Link to published version (if available):
10.1016/j.jcis.2014.12.040

Link to publication record in Explore Bristol Research
PDF-document

A molecular framework for modelling the surface tensions and surface excesses of dilute surfactant solutions

Carmelo Herdes,[1] Olga Lobanova,[1] Erik E. Santiso,[1, 2] George Jackson,[1] Julian Eastoe,[3] Craig James[3] and Erich A. Müller[1, *]

[1]*Department of Chemical Engineering, Imperial College London, South Kensington Campus, London, SW7 2AZ, U.K.*

[2]*School of Chemistry, University of Bristol, Bristol BS8 1TS, U.K.*

[3]*Department of Chemical and Biomolecular Engineering, North Carolina State University, Raleigh, NC, U.S.A.*

* corresponding author e.muller@imperial.ac.uk

Abstract

The straightforward molecular modelling of an aqueous surfactant system at concentrations below the critical micelle concentration (pre-cmc) conditions is unviable in terms of the presently available computational power. Considering a typical non-ionic surfactant, a fully atomistic simulation that includes several micelles will require in excess of $O(10^7)$ atom sites and several nanoseconds of real time. Here, we present an alternative that combines experimental information with simulations of a more modest size to understand the surface tension changes with composition and the structural behaviour of surfactants at the water-air interface. The crux of the matter is to express the surface tension as a function of the surfactant surface excess both in the experiments and in the simulations, allowing direct comparisons to be made. As a proof of concept a coarse-grained model of tetraethylene glycol monodecyl ether is considered at the air-

water interface at 298 K, with a force field parameterized through an equation of state (SAFT-γ-Mie). An excellent agreement is obtained between the simulation results and experimental observations in terms of efficiency and effectiveness.

Keywords: Molecular dynamics, molecular simulation, coarse graining, non-ionic amphiphiles, $C_{10}EO_4OH$

1.   Introduction

Surface tension is the utmost property of interest in solutions of surfactants and amphiphiles, and knowledge of its behaviour as a function of temperature, pressure and concentration is a key factor to evaluate the performance of consumer household products, biocompatible drug delivery systems, additives for enhanced gas solubility and oil recovery, just to name a few.[1,2] (delete this – it is not true ~~The reduction of the air-water surface tension is ultimately related to the capacity of amphiphilic molecules of self-assembling into micellar structures and mesophases, which often are the base of their utilization~~.)

The capacity of a surfactant for lowering the surface tension of an aqueous solution can be discussed in terms of (i) the concentration required to produce a given surface tension reduction and (ii) the maximum reduction in surface tension that can be obtained regardless of concentration.[3] These are referred to as the surfactant efficiency and effectiveness respectively. As a rule of thumb, a good measure of the surfactant adsorption efficiency is the concentration of surfactant required to produce a 20 mN m^{-1} reduction in surface tension. At this value, typically the surfactant concentration is close to the minimum concentration needed to produce maximum adsorption at the interface. The maximum surface excess generally lies in the range $1 - 4.4 \times 10^{-10}$ mol cm^{-2} (see

comment below) .[4] The performance of a given surfactant can also be discussed in terms of effectiveness of adsorption at the air-water interface. The effectiveness of adsorption is an important factor in determining such properties as foaming, wetting, and emulsification. This is usually defined as the maximum lowering of surface tension γ_{min} (regardless of concentration), or as the surface excess concentration at surface saturation equivalent to the maximum adsorption, Γ_{max}, a measure of the interfacial packing. For non-ionic surfactants, γ_{min}, and Γ_{max}, happen to closely match at what is called the critical micelle concentration[2] (cmc), the point in which a surface phase transition occurs and surfactants self-assemble in the bulk water phase. The efficiency and effectiveness of surfactants do not necessarily run parallel, and it is commonly observed – as shown by Rosen's extensive data listing[3] – that materials producing significant lowering of the surface tension at low concentrations (i.e., they are more efficient) have smaller Γ_{max} (i.e., they are less effective).

At the molecular level, surfactant efficiency is mainly dictated by the energetics while its role in effectiveness is directly related to entropic effects, i.e. to the relative size of the hydrophilic and hydrophobic portions of the adsorbing molecule. The area occupied by each molecule is determined either by the hydrophobic chain cross-sectional area, or the area required for closest packing of head groups, whichever is greater. Therefore, surfactant films can be tightly or loosely packed resulting in very different interfacial properties. For instance, straight chains and large head groups (relative to the tail cross section) favour close, effective packing, while branched, bulky, or multiple hydrophobic chains give rise to steric hindrance at the interface. This competition between energetic and entropic contributions may lead to the observation of surface phase transitions at the interfaces,[5] including liquid crystal-like dense 2D phase upon compression. On the other hand, within a series of single straight chain

surfactants, increasing the hydrocarbon chain length from C_8 to C_{20} will have little effect on adsorption behaviour.[3]

It is a non-trivial task to deduce the mesophase behaviour of dilute surfactants solutions, hence the increased relevance on experimental probing of these systems. Simple experimental approaches can be implemented for the measurement of the air-water surface tensions in dilute surfactant solutions; however, they only provide indirect evidence of the surface filling by surfactants. On the other hand direct scattering methods (e.g. neutron reflection) are routinely used to probe the surfactant layer structures and self-assembly at the water-air interfaces.[6]

It would seem sensible to interrogate these systems employing molecular simulation. For recent reviews of the current perspective on the applications of molecular modeling in the present context the reader is referred to the reviews by Gubbins et al.,[7] Maginn and Elliott[8] and in particular to the recent one by Creton et al.[9] , focused on surfactant solutions. The straightforward atomistic modelling of a surfactant system at pre-cmc conditions is unviable in terms of the present (and foreseeable future) computational capacity; as an example, consider a typical non-ionic surfactant, which ca. 60 atoms immersed in water. The concentrations range in the pre-cmc region span from zero up to O $(10^{-4}$ mol dm$^{-3})$[4] . The smallest simulation cell to mimic the latter state point must have almost 100 000 water molecules per surfactant. If one wishes to model the saturated surface along with single surfactants in the bulk and/or several micelles then the system size runs into the $O(10^7)$ atom sites. Furthermore, to guarantee an equilibrated state and suitable statistics, simulations need to be run for at least several hundreds of nanoseconds to explore the diffusion dynamics. This is not within the realm of the simulations possible in terms of *both* system size and simulation length. The most discouraging point is that in this scenario, due to the dilution of the system, the vast

majority of the computations are spent in modelling the bulk behaviour of pure water, which, in this context, is superfluous.

It is not to say that "heroic" atomistic simulations have not been attempted to study a variety of surfactant micellar systems[10, 11, 12, 13, 14, 15, 16, 17, 18, 19, 20, 21, 22] and insights have been gained regarding structural properties of post-cmc regions through calculation of density distributions, micelle size and shapes, average micellar population, etc. The challenge remains in tackling computationally demanding calculations in the pre-cmc region. Coarse-grained (CG) methodologies been used to approach these systems, reducing the number of non-relevant degrees of freedom and allowing for a more tractable simulation,[23, 24, 25, 26, 27, 28, 29, 30] . However, even with commonly used CG approaches, pre-cmc calculations are strongly dependent on (i) the capability of the model to preserve the molecular character of surfactant-solvent interactions and, (ii) the adopted methodology.[31,32,33,34,35,36,37,38,39] {EAM: to review these references}

The aim of this communication is to present an alternative simulation method to explore the pre-cmc region in a surfactant at the free air-water interface. Having an experimental setup in mind we propose the use of a representative simulation cell to model this system in a tractable time span based on the calculation of the surface tension in terms of the surface excess data. The key point of this set up is to recognize that in the dilute regime, the concentration of the surfactant in the bulk solution is negligible as compared to the accumulation at the free surface and that the accounting of the bulk phase adds no new information ~~to the study~~.

2.   Surface tension isotherms

Experimentally, the outcome of tensiometry is the generation of a surface tension isotherm, data giving the variation of surface tension with concentration. The plot will typically have a shape similar to that seen in the left hand side of figure 1. The tension decreases with concentration until a limiting value is obtained, where the increase in surfactant concentration does not alter the tension. The challenge from a molecular simulation perspective is to model this curve, as the concentrations involved are in a very dilute regime.

In terms of classical thermodynamics, the Gibbs adsorption isotherm expresses the relationship that must hold at a given at a constant temperature and pressure between the surface tension, the chemical potential, μ_I , and number of moles , n_i^s, of the k components within an arbitrary region defined as an interface, s, that separates two bulk regions α and β,

$$\sum_{i=1}^{k} n_i^s dm_i + Adg = 0 \qquad (1)$$

It is convenient to express the compositions in terms of an intensive quantity, the surface excess, Γ, defined as

$$G_i = \frac{n_i^s}{A} = \frac{n_i^{total} - n_i^a - n_i^b}{A} \qquad (2)$$

For a binary system consisting of a solvent (1), and a solute (2), equation (2) reduces to

$$-dg = G_1 dm_1 + G_2 dm_2 \qquad (3)$$

considering the choice of the Gibbs dividing surface position, so that $\Gamma_1 = 0$, then equation (4) simplifies to

$$dg = -G_2 dm_2 \qquad (4)$$

For simplicity we drop here the indices and take Γ to be the surfactant surface concentration at the air-water interface.

It can be safely assumed that a dilute solution complies with ideal solution behaviour hence $dm = RT\,d\ln(c)$ were R is the gas constant, T is the system temperature and c is the surfactant concentration, then we can rewrite (4) as:

$$G = -\frac{1}{RT}\frac{dg}{d\ln(c)} \qquad (6)$$

Equation (6) relates the surfaces excess to the derivative of the surface tension isotherm. Hence, one could use the isothermal data in the pre-cmc region where tangents of the plot correspond to $(\frac{d\gamma}{d\ln(c)})$, and can be used to obtain to produce a curve that relates the surface excess to the bulk surfactant concentration ($c.f.$ figure 1 top right) . Experimentally, this procedure has been proved to work well for C_iE_jOH nonionic surfactants, finding good agreements between Γ values from tensiometry and using (6)[9] with those measured directly by neutron reflection.[5]

However, a more interesting plot is that of the surface tension in terms of the surface excess, which again is acquired from the same data. The novelty of the methodology used herein is found in the actual abstraction for the construction of the simulation cell, based on exploring Γ rather than surfactant concentration.
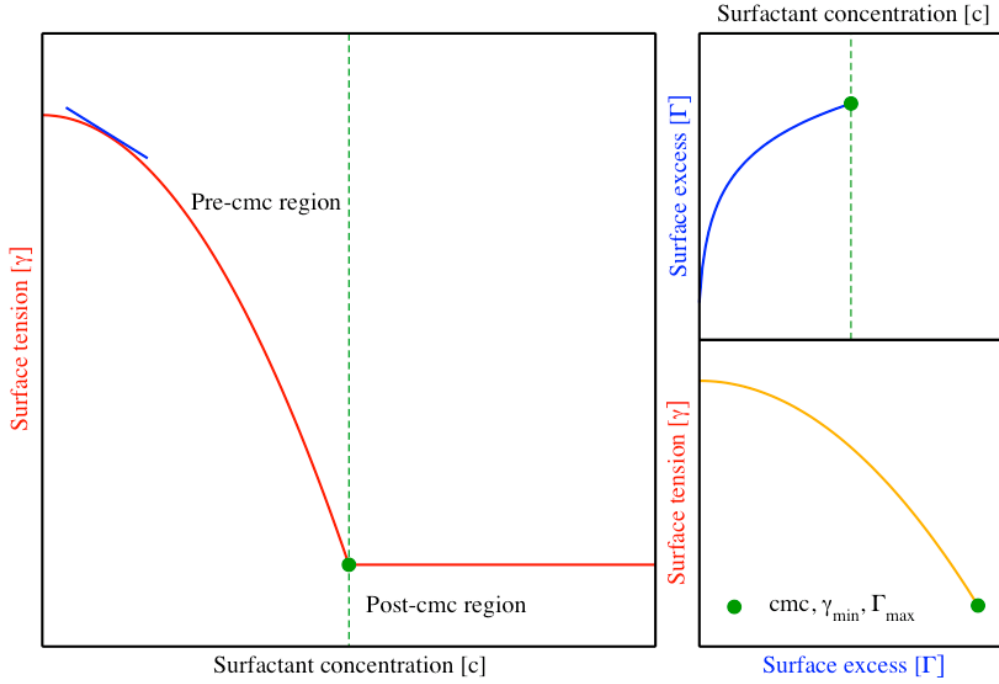
Figure 1. Schematic representation of surface tension as a function of surface excess. Details are found in the main text.

In a canonical (constant number of particles, volume and temperature) ensemble, one may calculate the surface tension, γ, directly from a molecular dynamics simulation. There are essentially two routes to the determination of the surface tension, the most common one explores the relationship elements of the pressure tensor, or mechanical route. A recent development consists of relating the tension to the results of a perturbation approach, sometimes referred to as the thermodynamic route[40]. In the limit of a planar interface both methods yield identical results.[41] In most "off the shelf" MD programs, the components of the pressure tensor, P_{ii} are calculated explicitly using the virial (mechanical) route, hence its use herein. Assuming a two phase system with a clear interface, the tension is proportional to the difference between the normal (z direction) and the tangential components (x-y direction) of the pressure tensor:

$$g = \frac{1}{n} \int_0^{Lz} \left[P_{zz} - \frac{P_{xx} + P_{yy}}{2} \right] dz \qquad (5)$$

where L_z is the longest length of the simulation cell and n is the number of surfaces.[38]

From the molecular dynamics perspective a direct calculation of the equilibrium surface tension as a function of the surface excess can be performed independently of the surfactant concentration. Since the system is very dilute (bulk concentrations are typically in the order of 10^{-4} mol dm^{-3}) in a small simulation cell, the number of free surfactants in solution away from the interface is negligible. Hence one can focus on the number of molecules on the surface, which in essence will be numerically equivalent to Γ, from where the bottom-right-hand plot in figure 1 can be drawn.

3.   Molecular dynamics details.

As a proof of concept, we consider the non-ionic surfactant tetraethylene glycol monodecyl ether ($C_{10}EO_4OH$, CAS Number 5703-94-6) at the air-water interface at 298 K. Experimental data report a surface tension variation from 72 to 28 mN m^{-1} when the surfactant bulk concentration goes from zero to the cmc at 6.1×10^{-4} mol dm^{-3}, respectively.[42]

We chose to coarse grain the surfactant in order to access both the time and length scales required for the modelling of the system. Within this reduction in the degrees of freedom of the system, a single isotropic bead is used to describe two water molecules[43]. Although several options are available for choosing the number of water molecules in a CG bead[44], this choice guarantees that the parameterization produces densities, tensions, vapour pressures and melting points close to the experimental values. Surfactant molecules were recast at the same level of definition by employing tangent-beads, a double bead labelled OA, which groups the terminal -[CH_2-O-CH_2-CH_2-OH], a bead labelled EO, for the groups -[CH_2-O-CH_2]- and a CM bead representing either the –[CH_2-CH_2-CH_2]- or the terminal –[CH_2-CH_2-CH_3] groups.

Figure 2 shows a cartoon of the CG model and a superimposed atomistic depiction for reference purposes only.
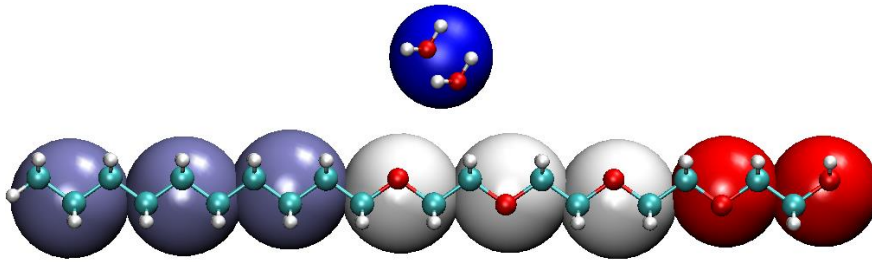
Figure 2. A cartoon of the CG model. Blue beads are CM (alkane-like), white are the EO (ethoxylated-like) and red are the AO (alcohol-like) coarse grained beads. The underlying atomistic depiction is placed as a reference, although the force field parameters are not obtained from the atomistic model, but from a top-down approach.

The parameterization was carried out using SAFT-γ Mie approach, where the non-bonded parameters for each group were obtained by fitting to macroscopic properties of the molecules regarding different functionalities. The SAFT equation of state is a perturbation approach based on a well-defined Hamiltonian, hence the CG beads are represented in the theory by a Mie potential, u,

$$u(r) = \left(\frac{\lambda_r}{\lambda_r - \lambda_a}\right)\left(\frac{\lambda_r}{\lambda_a}\right)\varepsilon\left[\left(\frac{\sigma}{r}\right)^{\lambda_r} - \left(\frac{\sigma}{r}\right)^{\lambda_a}\right] = Ar^{-\lambda_r} - Cr^{-\lambda_a} \qquad (6)$$

where r is the intermolecular distance, and ε, and σ, and are the adjustable parameters relating to the energy and distance scales. Noteworthy is that while the dispersion exponent was fixed at the value of six, the short-range repulsion (λ_r) adopted different values reflecting the average softness/hardness of the potential. More details about this procedure can be found elsewhere. [45,46,47,48,49] The Mie potential in (6) may expressed in terms of two constants A and C that consolidate all the functionality corresponding to the prefactor and the size and energy parameters. This functional form, expressed in the right hand side of equation (6) is commonly used when tabulating potentials in MD codes. The intramolecular parameters describing the structure and rigidity of the

surfactant molecules are obtained by an analysis of single component molecules[50]. The intramolecular interactions are described by a harmonic potential that accounts for bond angle bending between three adjacent beads,

$$U_{intra} = \overset{Angle}{\sum} k_a \left(q - q_0\right)^2 \tag{7}$$

where $k_a = 2.1113$ [kcal/mol/rad^2] is the bending spring constant and $\theta_0 = 157.6°$ is the equilibrium angle. The distance between the beads is kept rigidly to σ. In practice, a stiff spring can be used to represent this bond distance. Table 1 summarizes the selected coarse-grained parameters.

Table 1. Non-bonded coarse-grained parameters.

Interaction	σ [nm]	ε/k_B [K]	λ_r	C [kJ mol^{-1} nm^6]	A [kJ mol^{-1} nm^λ_r]
OA-OA	0.37244	461.11	19.00	2.54587E-02	6.75412E-08
OA-EO	0.38929	392.00	19.00	2.82219E-02	1.33066E-07
OA-CM	0.40440	375.50	16.86	3.75230E-02	2.02126E-06
OA-W	0.37352	492.00	11.94	4.47232E-02	1.28300E-04
EO-EO	0.40613	396.90	19.00	3.68439E-02	3.01309E-07
EO-CM	0.42124	352.00	16.86	4.49336E-02	3.76974E-06
EO-W	0.39036	480.00	11.94	5.68529E-02	2.11993E-04
CM-CM	0.43635	344.42	15.00	6.06844E-02	3.48010E-05
CM-W	0.40547	250.00	10.75	4.36947E-02	6.02313E-04
W-W	0.37459	399.96	8.00	8.71139E-02	1.22238E-02

Remove the "E" number notation – use standard scientific notation

For the description of the pre-cmc region, a parallelepiped simulation box with aspect ratio $L_z/L_x = 6$ was used, where $L_x=L_y=$ 6 nm. 16000 (8000 CG beads) water molecules were employed, and the number of surfactant molecules was varied from 1 to 96 per surface. This unit cell, initially filled with water molecules, is much larger than the one needed for a pure liquid phase; hence a slab of liquid is stabilized and coexists with a water vapour phase. At these conditions, the density of the water vapour is several orders of magnitude less than that of the liquid; hence is in essence a vacuum. Surfactant molecules were initially placed randomly in the void spaces of the cell, but rapidly migrated and collected at the surfaces of the aqueous slab. Larger systems with $L_x=L_y=$ 12 nm and 64000 water molecules were tested with no appreciable difference in the results.

The system was run under a molecular dynamics canonical (NVT) ensemble, where the total volume, concentration and temperature are kept constant. The simulations were thermostated to 298K every 1ps by a Nose-Hoover algorithm, all non-bonded interactions were truncated at 2.0 nm. The GROMACS simulation open source suite[51] was used to calculate the molecular dynamics. The systems were run with a timestep of 0.01 ps for at least 20 ns. It should be noted that due to the CG nature of the forcefields, the dynamics of the system is also accelerated, hence 20 ns would correspond to a simulation of roughly 0.2 μs if an all atom approach would have been used[52]. All reported properties came from relevant averages, taken over the last half of the configurations explored.

4.   Results and discussions

Figure 3 shows a prediction of the surface tension in comparison with the experimental data.[9] On the approach to the maximum surface concentration, surfactant

molecules are eventually driven from the interface and explore the bulk water region. This shows up as a surface roughness, as can be seen in figure 4. The surface tension is monotonically decreased as more surfactant molecules reach the interface. A critical point is reached when the concentration of surfactants at the surface reaches $\Gamma_{max} = 4.43$ $x10^{-6}$ mol m^{-2} (you have mixed units here sometimes mol m^{-2} other times mol cm^{-2} – please homogenise units) corresponding to 96 surfactant molecules per surface in the periodic cell). A this point any further increase in the number of molecules results in the formation of micelles that eventually detach from the surface and explore the bulk water. The maximum surface excess is in excellent agreement with the experimental[9] value at 4.07 $x10^{-6}$ mol m^{-2}. It is important to point out that if larger concentrations are considered the system will surpass the cmc and some of the surfactant molecules will be in micelles in the bulk region. An (erroneous) application of eq. (5) in this state point will give a numerical result for the tension, however, it would be an error to consider this point in the surface excess plot (figure 3), as the multiple interfaces formed by the micelles would be affecting the calculation of the pressure tensors. The final saturation point of the system cannot be deduced without either visually inspecting the configurations to rule out the formation of micelles, or by monitoring the positions of the surfactant molecules in the simulation box.
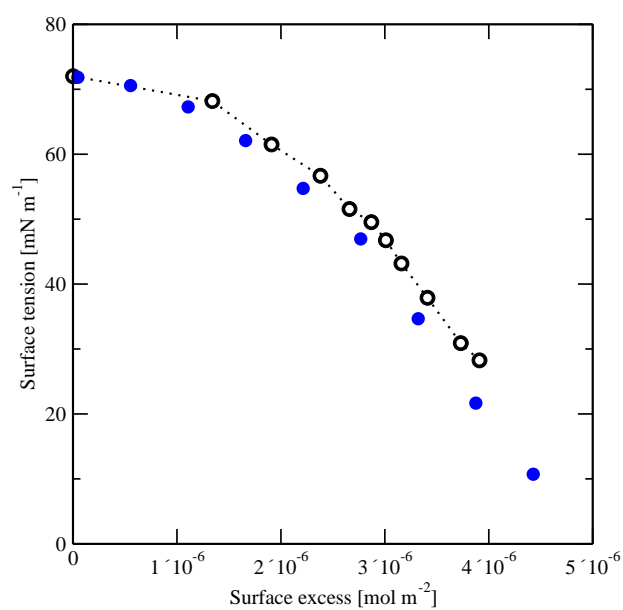
Figure 3. Surface tension as a function of surface excess, simulation prediction (blue solid circles) in comparison with experimental data (black open circles).[9]
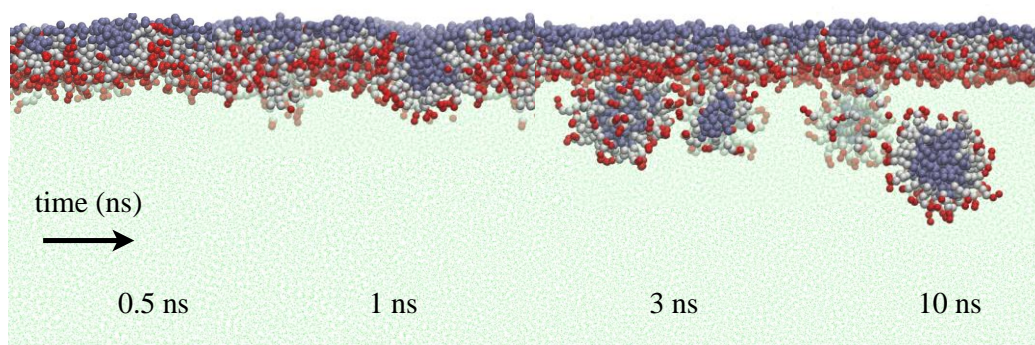
Figure 4. Snapshot sequence of the time evolution of the formation and separation of micelles from a surface with an initial surfactant concentration above the maximum surface concentration. The state shown corresponds to 4.98 x10-6 mol.m^{-2} or 216 surfactant molecules in a periodic cell.
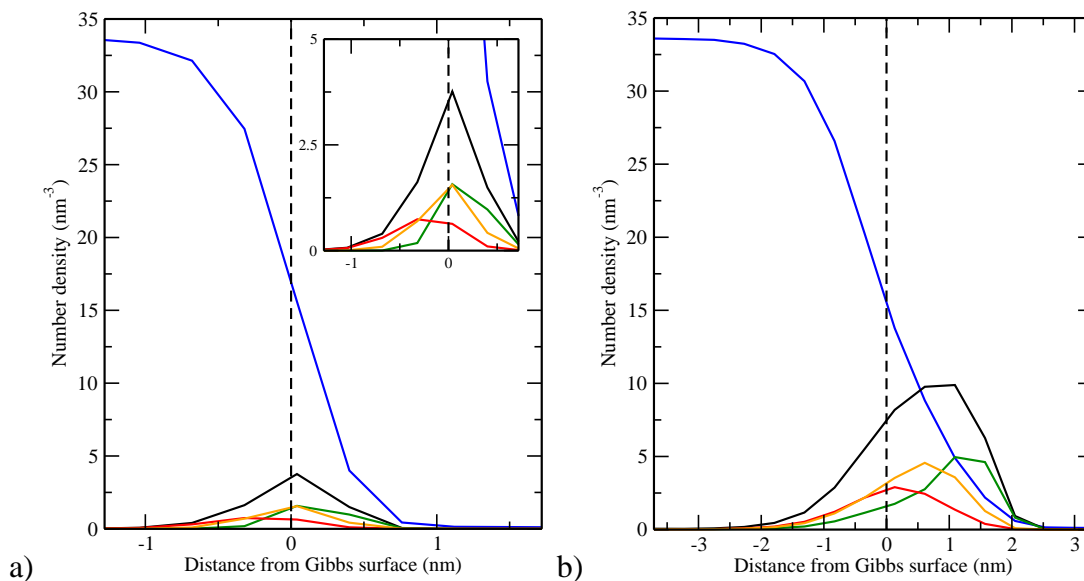
Figure 5. Density profiles of the different bead types as a function of the distance to the Gibbs dividing surface, as defined by the water molecules. Colored lines stand for blue, water; black, surfactant COM; red, OA; orange, EO and green, CM. Left corresponds to a sparse surface coverage, while right corresponds to a point close to the maximum coverage.

In this sense, the simulations allow the monitoring of molecular conformations at the interface. Figure 5a and b, present concentration profiles of the different individual beads and oc the center of mass (COM) of surfactant molecules perpendicular to the *xy* plane for a surface coverage of 0.275×10^{-6} mol m^{-2} and 2.035×10^{-6} mol m^{-2}, respectively. The dashed line corresponds to the Gibbs dividing surface, as defined by the water profile. It can be seen how upon approach to saturation the centre of mass displaces towards the air-water interface. These types of curves bring detailed information, that help understand the role of each component of the surfactant on the surface at a given coverage in the pre-cmc region.

It is worth reaffirming that the simulations as reported are incapable of determining the actual concentration of the cmc. It is here that a link to experiments must be made, i.e. by mapping the surface excess in both the model and the experiment.

5.   Conclusions

We present an alternative simulation method to explore the pre-cmc region of a surfactant at the air-water interface, based on the calculation of the surface tension in terms of the surface excess values. Although simulations of this type, where a given number of surfactants are places in a periodic box with an water-vapor interface are not uncommon, there is no systematic way of relating simulations to the more common adsorption isotherms. The use of the surface excess as a characteristic measure of interfacial concentration has the advantage that it can be directly calculated in simulations and inferred with confidence from experiments.

The use of physically-based coarse grained approaches, such as the SAFT-γ forcefield, not only allow for the exploration of meaningful system sizes and times, but also provides quantitative predictions in terms of the efficiency and effectiveness of aqueous surfactant solutions.

Just my comments to Erich about boosting/amplifying this section with reference to published literature

Cover art:
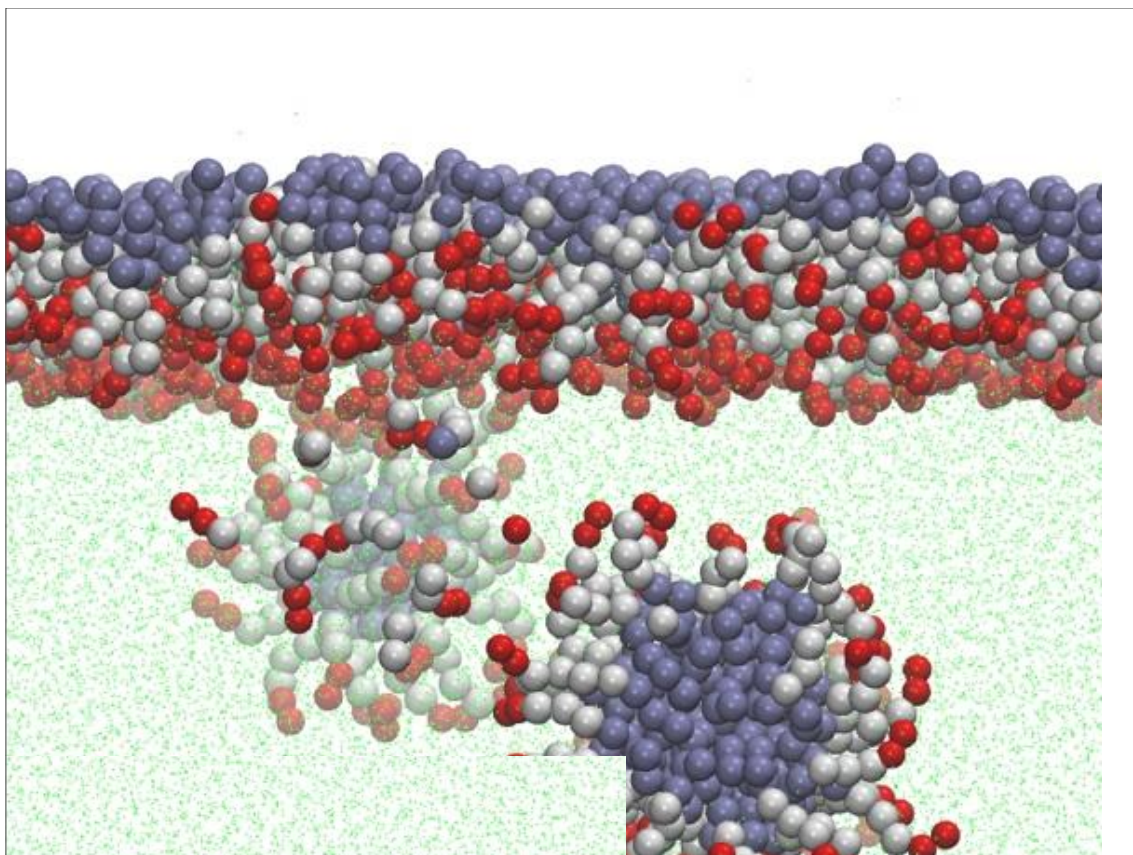
References { CH: to fix the reference style when the journal has been selected}

1   J.N. Israelachvili, Intermolecular and surface forces, 2nd ed. (Harcourt Brace, London 1992).

2   D. R. Karsa, Industrial applications of surfactants IV. Cambridge: RSC, 1999

3   J. Eastoe, (2009) Surfactant Aggregation and Adsorption at Interfaces, in Colloid Science: Principles, Methods and Applications (ed T. Cosgrove), Blackwell Publishing Ltd., Oxford, UK.

4   M.J. Rosen and J.T. Kunjapp, (2012) Surfactants and Interfacial Phenomena, 4th ed., John Wiley & Sons, USA.

5   D. Vollhardt and V.B. Fainerman, Characterisation of phase transition in adsorbed monolayers at the air/water interface, *Advances in Colloid and Interface Science* **2010**, *154*, 1–19.

6   J Eastoe, J.S Dalton, Dynamic surface tension and adsorption mechanisms of surfactants at the air–water interface, Adv. Coll. Interf. Sci. 85, 103–144, (2000)

7   Gubbins, K. E., Liu, Y. C., Moore, J. D., and Palmer, J. C. The role of molecular modeling in confined systems: Impact and prospects. *Physical Chemistry Chemical Physics* **2011**, *13*(1), 58-85

8   E J. Maginn and J. R. Elliott, Historical Perspective and Current Outlook for Molecular Dynamics as a Chemical Engineering Tool, Industrial and Engineering Chemistry Research, 2010, 49, 3059-3078

9   B. Creton, C. Nieto-Draghi and N. Pannacci, Prediction of Surfactants' Properties using Multiscale Molecular Modeling Tools: A Review *Oil & Gas Science and Technology – Rev. IFP Energies nouvelles,* Vol. 67 (2012), No. 6, pp. 969-982

10   E.S. Boek, A. Jusufi, H. Lowen, G.C. Maitland, Molecular design of responsive fluids: molecular dynamics studies of viscoelastic surfactant solutions, J. Phys. Condens. Matter 14 (2002), pp. 9413 – 9430.

11   B. Jonsson, O. Edholm, O. Teleman, Molecular-dynamics simulations of a sodium octanoate micelle in aqueous-solution, J. Chem. Phys. 85 (1986), pp. 2259 – 2271.

12   K. Watanabe, M. Ferrario, M.L. Klein, Molecular-dynamics study of a sodium octanoate micelle in aqueous-solution, J. Phys. Chem. 92 (1988), 819 – 821.

13   K. J. Schweighofer, U. Essmann, M. Berkowitz, Simulation of sodium dodecyl sulfate at the water-vapor and water-carbon tetrachloride interfaces at low surface coverage, J. Phys. Chem. B 101 (1997), 3793 – 3799.

14   J.B. Maillet, V. Lachet, P.V. Coveney, Large scale molecular dynamics simulation of self-assembly processes in short and long chain cationic surfactants, Phys. Chem. Chem. Phys. 1 (1999), 5277 – 5290.

15   D.P. Tieleman, D. van der Spoel, H.J.C. Berendsen, Molecular dynamics simulations of dodecylphosphocholine micelles at three different aggregate

sizes: Micellar structure and chain relaxation, J. Phys. Chem. B 104 (2000), 6380 – 6388.

16 S.J. Marrink, D.P. Tieleman, A.E. Mark, Molecular dynamics simulation of the kinetics of spontaneous micelle formation, J. Phys. Chem. B 104 (2000), 12165 - 12173.

17 J. Shelley, K. Watanabe, M.L. Klein, Simulation of a sodium dodecyl-sulfate micelle in aqueous-solution, Int. J. Quantum Chem. 38 (1990), 103 - 117.

18 A.D. MacKerell, Molecular-dynamics simulation analysis of a sodium dodecyl-sulfate micelle in aqueous-solution - decreased fluidity of the micelle hydrocarbon interior, J. Phys. Chem. 99 (1995), 1846 – 1855.

19 Bast, T.; Hentschke, R. Molecular dynamics simulation of a micellar system J. Mol. Model. 1996, 2, 330.

20 Bruce, C. D.; Berkowitz, M. L.; Perera, L.; Forbes, M. D. E. Molecular dynamics simulation of sodium dodecyl sulfate micelle in water: Micellar structural characteristics and counterion distribution J. Phys. Chem. B 2002, 106, 3788.

21 Rakitin, A. R.; Pack, G. R. Molecular dynamics simulations of ionic interactions with dodecyl sulfate micelles J. Phys. Chem. B 2004, 108, 2712.

22 Yoshii, N.; Okazaki, S. Chem. A molecular dynamics study of surface structure of spherical SDS micelles Phys. Lett. 2006, 426, 66.

23 Sammalkorpi, M.; Karttunen, M.; Haataja, M. Structural properties of ionic detergent aggregates: a large-scale molecular dynamics study of sodium dodecyl sulfate J. Phys. Chem. B 2007, 111, 11722.

24 Cheong, D. W.; Panagiotopoulos, A. Z. Monte Carlo simulations of micellization in model ionic surfactants: Application to sodium dodecyl sulfate Langmuir 2006, 22, 4076.

25 Gelbart, W. M.; BenShaul, A. The "new" science of "complex fluids" J. Phys. Chem. 1996, 100, 13169.

26 Goetz, R.; Lipowsky, R. Computer simulations of bilayer membranes: Self-assembly and interfacial tension J. Chem. Phys. 1998, 108, 7397.

27 Bandyopadhyay, S.; Klein, M. L.; Martyna, G. J.; Tarek, M. Molecular dynamics studies of the hexagonal mesophase of sodium dodecylsulphate in aqueous solution Mol. Phys. 1998, 95, 377.

28 Shelley, J. C.; Shelley, M. Y. Computer simulation of surfactant solutions Curr. Opin. Colloid Interface Sci. 2000, 5, 101.

29 Marrink, S. J.; de Vries, A. H.; Mark, A. E The binary mixing behavior of phospholipids in a bilayer: A molecular dynamics study J. Phys. Chem. B 2004, 108, 750.

30 Gao, J.; Ge, W.; Hu, G.; Li, J. From homogeneous dispersion to micelles - A molecular dynamics simulation on the compromise of the hydrophilic and

hydrophobic effects of sodium dodecyl sulfate in aqueous solution Langmuir 2005, 21, 5223.

[31] Shinoda, W.; DeVane, R.; Klein, M. L. Multi-property fitting and parameterization of a coarse grained model for aqueous surfactants Mol. Simul. 2007, 33(1-2), 27.

[32] Mohan, G.; Kopelevich, D. I. A multiscale model for kinetics of formation and disintegration of spherical micelles, J. Chem. Phys. 2008, 128, 044905.

[33] Sterpone, F.; Briganti, G.; Pierleoni, C. Sphere versus Cylinder: The Effect of Packing on the Structure of Nonionic C12E6 Micelles, Langmuir 2009, 25, 8960.

[34] Alexandridis, P.; Holzwarth, J. F.; Hatton, T. A. Interfacial Dynamics of Water-in-Oil Microemulsion Droplets - Determination of the Bending Modulus using Iodine Laser Temperature-Jump Langmuir 1993, 9, 2045.

[35] A. Jusufi, S. Sanders, M.L. Klein, A.Z. Panagiotopoulos, Implicit-solvent models for micellization: Nonionic surfactants and temperature-dependent properties, J. Phys. Chem. B 115 (2011), pp. 990–1001.

[36] Bandyopadhyay, S.; Tarek, M.; Lynch, M. L.; Klein, M. L. Molecular dynamics study of the poly(oxyethylene) surfactant C12E2 and water Langmuir 2000, 16, 942.

[37] Sterpone, F.; Briganti, G.; Pierleoni, C. Molecular dynamics study of spherical aggregates of chain molecules at different degrees of hydrophilicity in water solution Langmuir 2001, 17(16), 5103.

[38] Garde, S.; Yang, L.; Dordick, J. S.; Paulaitis, M. E. Mol. Phys. 2002, 100(14), 2299.

[39] Shinoda, W.; DeVane, R.; Klein, M. L. Coarse-grained molecular modeling of non-ionic surfactant self-assembly Soft Matter 2008, 4(12), 2454.

[40] G. J. Gloor, G. Jackson, F. J. Blas, and E. de Miguel Test-area simulation method for the direct determination of the interfacial tension of systems with continuous or discontinuous potentials J. Chem. Phys. 123, 134703 (2005)

[41] Sampayo JG, Malijevský A, Müller EA, de Miguel E, Jackson G Communications: Evidence for the role of fluctuations in the thermodynamics of nanoscale drops and the implications in computations of the surface tension. J Chem Phys. (2010) 132, 141101

[42] J. Eastoe, J.S. Dalton, P.G.A. Rogueda, E.R. Crooks, A.R. Pitt, and E.A. Simister, Dynamic surface tension of nonionic surfactant solutions, J. Colloid Interface Sci. 188 (1997), pp. 423 – 430.

[43] Lobanova O, Avendaño C , Lafitte T, Jackson G , Müller EA. 2013. SAFT-gamma force field for the simulation of molecular fluids. 4. Coarse grained models for water in preparation

[44] K. R. Hadley and C. McCabe On the Investigation of Coarse-Grained Models for Water: Balancing Computational Efficiency and the Retention of Structural Properties J Phys Chem B. (2010) 114: 4590–4599.

[45]   C. Avendaño, T. Lafitte, A. Galindo, C.S. Adjiman, G. Jackson, E.A. Müller, SAFT-gamma force field for the simulation of molecular fluids. 1. A single-site coarse grained model of carbon dioxide, J. Phys. Chem. B 115, 38 (2011), pp. 11154 – 11169

[46]   Avendaño C, Lafitte T, Adjiman CS, Galindo A, Müller EA, Jackson G., SAFT-γ Force Field for the Simulation of Molecular Fluids: 2. Coarse-Grained Models of Greenhouse Gases, Refrigerants, and Long Alkanes, J Phys Chem B. 2013, 117:2717-33

[47]   T. Lafitte, C. Avendaño, V. Papaioannou, A. Galindo, C.S. Adjiman, G. Jackson, E.A. Müller, SAFT-gamma force field for the simulation of molecular fluids: 3. Coarse-grained models of benzene and hetero-group models of n-decylbenzene, Molecular Physics 110, 11-12 (2012), pp. 1189 – 1203.

[48]   Lobanova, O., Avendaño, C., Jackson, G., Müller, E. A. *In preparation*

[49]   EA Muller and G. Jackson Force Field Parameters from the SAFT-γ Equation of State for use in Coarse-Grained Molecular Simulation, *Ann. Rev. Chem . Biomol. Eng.* 5, (2014) *in press*

[50]   Rahman S, Lobanova O, Correia-Braga C, Raptis V, Müller EA, Jackson G. 2013. in preparation

[51]   D. Van Der Spoel, E. Lindahl, B. Hess, G. Groenhof, A.E. Mark, H.J. Berendsen, GROMACS: fast, flexible, and free, J. Comput. Chem. 26, 16 (2005), pp. 1701 – 1718.

[52]   S.J. Marrink, H.J. Risselada, S. Yefimov, D.P. Tieleman and A.H. de Vreis, The MARTINI Force Field: Coarse Grained Model for Biomolecular Simulations *J. Phys. Chem.* 2007, 111, 7812-7824